# Towards Automated Computational Discovery of Battery Materials

Xiang Feng, Qianfan Zhang*, Zhi Wei Seh*

X. Feng, Prof. Q. Zhang

School of Materials Science and Engineering, Beihang University, Beijing 100191, P. R. China. Email: qianfan@buaa.edu.cn

Prof. Z. W. Seh

Institute of Materials Research and Engineering, Agency for Science, Technology and Research (A*STAR), 2 Fusionopolis Way, Innovis, Singapore 138634, Singapore. Email: sehzw@imre.a-star.edu.sg

**Abstract**

New rechargeable batteries with high energy density and low cost have been intensively explored, but their commercialization still faces multiple challenges involving battery materials and interfaces. Some difficulties faced by battery materials are that a single material often needs to possess multiple functions, and also needs to be cheap, easy to prepare, safe and environmentally friendly. Recent developments in workflow managers (WMs) along with continuously increasing computing power have enabled the automated computational workflow method. Using this method, the WM can execute the predesigned research workflow to study tens of thousands of materials and screen out materials that meet the multiple requirements. In this perspective, we will present a critical overview of the automated computational workflows, focusing on the high-throughput study of battery materials. Firstly, an introduction to the automated computational workflow as well as commonly used WMs will be given. Next, the latest works and methods to build such automated workflows are presented. Finally, we provide an outlook on the existing challenges and future directions to drive computational and experimental developments in this nascent field.

## Introduction

The quest towards a sustainable energy future based on intermittent renewable energy warrants the need for efficient energy storage technologies.[1] Rechargeable batteries have the ability to store excess renewable energy and release it on demand to ensure a constant power supply. Lithium-ion batteries (LIBs) are the mainstream technology today for portable electronics, electric vehicles and grid storage owing to their reasonable energy density and cycle life.[2,3] Over the years, technologies beyond LIBs with higher energy density and lower cost have been intensively explored, but many are yet to be commercialized due to multiple challenges involving battery materials and interfaces.[4-6] Besides the anode, cathode and electrolyte materials, battery interfaces such as the anode-electrolyte and cathode-electrolyte interfaces are also equally important in determining the overall battery performance.

Why is the commercialization of new type of batteries so difficult? One of the main reasons may be that a single battery material often needs to achieve multiple functions at the same time.[7-15] As a typical example, lithium-sulfur batteries (LSBs) are still far from practical applications, even though they have been studied for decades as a promising candidate for next-generation rechargeable batteries. The main reason is that the cathode, anode, electrolyte, and the interfaces between them all face multiple challenges, and it is not easy to find materials that are cheap, simple to prepare, safe and environmentally friendly to overcome these challenges simultaneously. For example, the main challenges facing the sulfur cathode include low electronic and ionic conductivity, solubility of lithium polysulfides (LiPSs) and large volume change.[4,16] To solve the above-mentioned problems, the key is to find multifunctional sulfur hosts.[7-10] The lithium anode also faces multiple challenges of lithium dendrite growth and non-uniform formation of solid electrolyte interphase (SEI).[4,16] The electrolyte is even more complicated, since it is in contact with both the cathode and the anode. Although solid-state electrolytes (SSEs) can solve the flammable and volatile safety hazards of traditional organic liquid electrolytes, suppress the growth of lithium dendrites and prevent the dissolution of LiPSs, their lithium ion conductivities are often

several orders of magnitude lower than that of liquid electrolytes.[17,18] Effective SSEs need to be multifunctional with high lithium ion conductivity, suitable mechanical strength and large electrochemical window. Finally, the interfaces, as the connecting part between all battery materials, can be said to have a crucial impact on the overall performance of the battery. It can be predicted that the challenges faced by the interface are jointly determined by the two parts it connects, which means that the interfaces also need to be multifunctional.[14,15]

In fact, the commercialization of any battery system is bound to have many challenges due to its unique chemical and electrochemical processes.[19] To overcome these challenges, each battery material needs to perform multiple tasks. To find effective battery materials and interfaces, funnel-shaped screening workflow is a main method.[13,20] However, the application of the screening workflow currently relies largely on experimental trial-and-error to screen out the best material from a large number of candidate materials. Experiments are irreplaceable, but they do have disadvantages of being time-consuming, expensive, and low-throughput for screening. Compared with experiments, computational simulations are usually less time-consuming, cheaper, and easier to achieve high-throughput. Thus, it may be a more efficient method to firstly find several optimal materials from a large number of candidate materials through computational high-throughput screening, and then carry out experimental verification. Over the years, computer performance has grown rapidly in accordance with Moore's Law, and many computational material research groups have been able to perform high-throughput simulations. And the emergence of workflow managers (WMs) has provided a powerful tool for the above-mentioned computational high-throughput screening.[21] With the help of WMs, the construction of the computational screening workflow becomes much easier. The execution of the workflow becomes more efficient and automated, which requires minimum human intervention, and the reproducibility of research work is improved. Combining computational simulations with WMs, we propose a nascent but promising automated computational workflow method for the study of battery materials.

In this perspective, we will present a critical overview of the research in automated computational workflows with a focus on battery materials. We firstly introduce the automated computational workflow method and discuss how it works, how to build it, its advantages as well as commonly used WMs. Next, we will present the research works using this method in battery materials and some other fields. Finally, we also offer our perspectives on the unresolved problems and future directions to spur computational and experimental progress in this emerging field.

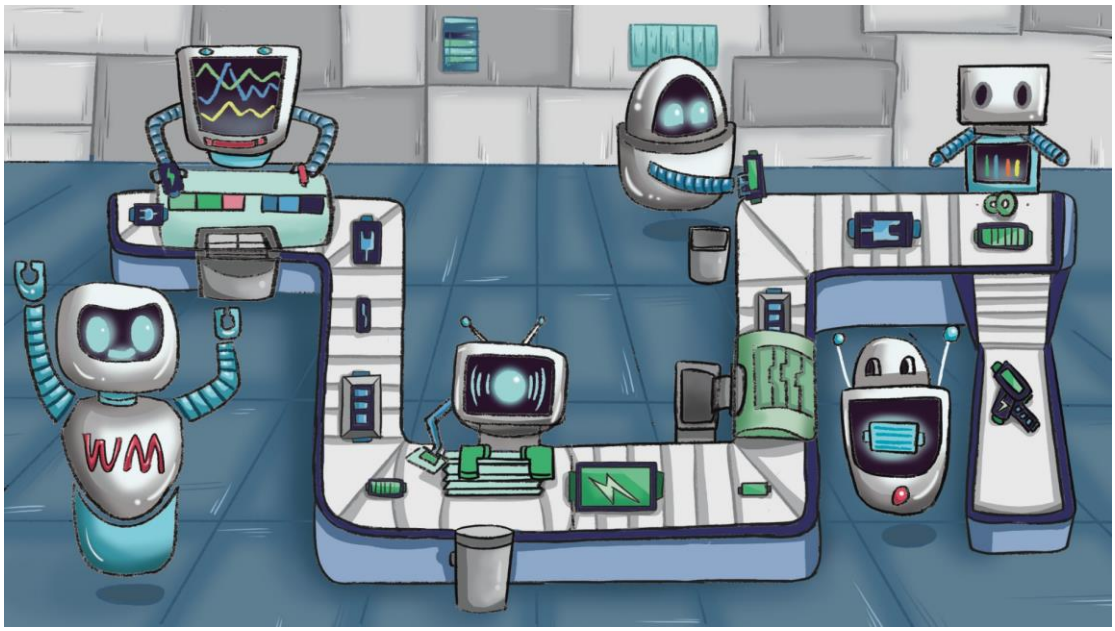


**Figure 1.** Automated computational workflow for battery materials discovery. The flow line represents a funnel-shaped battery material screening workflow, constructed by researchers using WM. According to the designed workflow, the WM will coordinate the simulation software, material database, computer cluster, job scheduler, and data analysis/visualization tools to screen battery materials together.

## Automated computational workflows

The so-called workflow, according to its literal meaning, is the order in which tasks are performed. Mathematically, a workflow can be described using a directed acyclic graph, which comprises two basic elements: vertex and edge. A vertex represents a task, and the direction of the edge connecting two vertices determines the execution order of two tasks. Judging whether a battery material satisfies the design strategy can be achieved

through a funnel-shaped screening workflow.[13,20] In such workflow, multiple properties of a material are simulated. Only if all these properties meet the requirements can it pass the screening. If a property fails to meet the requirements, this material will be eliminated immediately (see the flow line in **Figure 1**). To achieve the highest efficiency, a funnel-shaped screening workflow should follow a principle: the most accessible property should be simulated first and vice versa. An effective battery material has to possess good intrinsic properties, and its microstructure is of equal importance. For example, in the sulfur cathode of LSBs, the core-shell structure is adopted to confine $S_8$/$Li_2S$ in a conductive shell, which not only can inhibit the dissolution of LiPSs but also provide space for the volume change.[9,22-24] This means that the screening of battery materials will involve multi-scale simulations and corresponding software. The use of different simulation software follows a similar procedure, including the preparation of input files (e.g. material structures and simulation parameters), the execution of simulation software on computer clusters as well as the collection and analysis of results. In a high-throughput screening, the material structures are usually derived from material databases, and the simulation parameters are pre-specified by researchers. Since a computer cluster is often used by many users at the same time, the execution of simulation software on a computer cluster needs to be applied for and queued through a job scheduler. Finally, the collection and analysis of results can be realized by data analysis and visualization tools. In conclusion, a high-throughput screening workflow for battery materials is a combination of the inspiration of researchers, simulation software at different scales, material databases, computer clusters, job schedulers and data analysis/visualization tools. Thus, the manual execution of such high-throughput workflow is impractical. Thanks to the emergence of WMs, it provides a powerful tool for the construction and execution of such sophisticated workflow (Figure 1).

To build a workflow with a WM, firstly we need to analyze and decompose the overall workflow. Take the funnel-shaped screening workflow as an example. It can be simply regarded as a series of material property simulation tasks connected in terms of a

"progressive" logic. However, any property simulation cannot be completed in a single step, which means a property simulation is also a workflow. Since the property simulation is a part of the screening, we can call it a first-order sub-workflow of the screening workflow. In fact, this first-order sub-workflow may also be divided into many second-order sub-workflows. This decomposition process is repeated, until a high-order sub-workflow can be completed in a single step (e.g. file reading or writing). Such high-order sub-workflow can be called an atomic-workflow, indicating its indivisibility. Theoretically, no matter how complex a workflow is, it can be constructed by connecting a large number of atomic-workflows in terms of simple logic. But in practice, workflow construction does not need to be so cumbersome. WMs allow the encapsulation of commonly used workflows, so that they can be reused. Thus, in the process of workflow analysis and decomposition, as long as a sub-workflow has already been encapsulated before, it can be reused directly. In fact, some WMs have encapsulated a number of commonly used simulation workflows of popular simulation software, which further simplified the workflow construction. Once a workflow is constructed, the WMs can automate its execution to screen thousands of materials from the databases. When the workflow starts, the WMs will analyze the workflow graph, and submit tasks with no pre-task to the cluster through job schedular. When a task is completed, the WMs will analyze the graph again, and submit tasks whose pre-tasks have all completed. The above process is repeated until the workflow ends. The advantages are as follows: (1) the screening of multiple materials can be performed simultaneously; (2) the WMs can handle complex dependencies; (3) the WMs can execute a large number of concurrent tasks in a short period of time; (4) a workflow can be executed on multiple computer clusters with different job schedulers; (5) the workflow execution can be recorded in detail for a batter reproducibility; (6) excellent commonly used workflows can be encapsulated and shared, which can be reused directly by other researchers or be used as sub-workflows for the construction of more advanced workflows.

At present, the commonly used WMs include Automate,[25] AiiDA,[26,27] AFLOW,[28,29]

MyQueue,[30] Pipeline Pilot, etc. Automate (https://atomate.org) is based on open-source Python libraries pymatgen,[31] FireWorks,[32] and custodian. The Materials Project[33] database is powered by Automate. Automate not only can be used as a language to define dynamic workflows, but also provides many commonly used workflows such as the electronic band structure, elastic tensor and climbing-image nudged elastic band (CI-NEB) workflows. AiiDA (https://www.aiida.net) is an open-source WM written in Python. AiiDA can define dynamic workflows and the AiiDA engine owns the ability on sustaining high-throughput workloads involving tens of thousands of concurrent jobs per hour. AiiDA also has a detailed record of the workflow execution called the provenance graph. It is worth mentioning that the plugin module interfaces AiiDA with commonly used simulation software, such as VASP, Quantum ESPRESSO, LAMMPS and GROMACS. AFLOW (http://www.aflowlib.org) is a WM written in C++, which can automatically calculate various properties of materials. The material database AFLOWLIB[34] is powered by AFLOW. MyQueue (https://myqueue.readthedocs.io/en/latest) is an open-source front-end for job schedulers written in Python, which has a simple Python interface that can be used to define workflows. Pipeline Pilot (https://www.3ds.com/products-services/biovia/products/data-science/pipeline-pilot) is a commercial WM distributed by BIOVIA. Unlike WMs introduced above, when using the pipeline pilot as the WM, we build workflows through graphical user interface (GUI) rather than programming. Pipeline Pilot encapsulated complex functions in “components”. We can drag and drop these “components” and link them to build a workflow. It is worth mentioning that, many functions in BOVIA Materials Studio, the material design commercial software distributed by the same company, are also encapsulated as “components” for Pipeline Pilot to build workflows.

With the help of these WMs, automated computational workflows can become more intelligent. Due to unreasonable structures and simulation parameters, the simulation software may fail sometimes. If an error detecting and fixing sub-workflow is attached to each property simulation sub-workflow, the material screening will become more

stable and reliable. In fact, custodian is a Python library designed to detect and fix errors for simulation software.[25] The "aiida-simulation software" (e.g. aiida-vasp and aiida-lammps) plugins of AiiDA are also designed for the same purpose.[26,27] AFLOW can also identify various errors that occur during the operation of the simulation software, and actively correct them.[28,29] Besides, several new methods have been proposed that allow machines to make decisions that were previously only possible with human experience. These methods can be introduced as decision making sub-workflows, which makes the workflow more intelligent. For example, NEB is an important tool for the evaluation of the ionic conductivity of battery materials, but the ion transport path needs to be specified manually. In order to find the ion transport path with the lowest diffusion energy barrier, a large number of NEB calculations are required. He et al.[35-38] developed a method combining the crystal structure analysis by Voronoi decomposition (CAVD) method and the band valence site energy (BVSE) method. By analyzing the crystal structure, CAVD method can obtain the ion transport network and all possible ion transport paths. BVSE method, on the other hand, can predict the diffusion energy barrier on each ion transport path, thereby predicting the path with the lowest diffusion energy barrier. Using this method, one not only can save the trouble of manually path specifying, but also find the path with the lowest diffusion energy barrier directly to a large extent. Applying such method to an automated workflow will enable the rational decision making for the evaluation of the ionic conductivity.

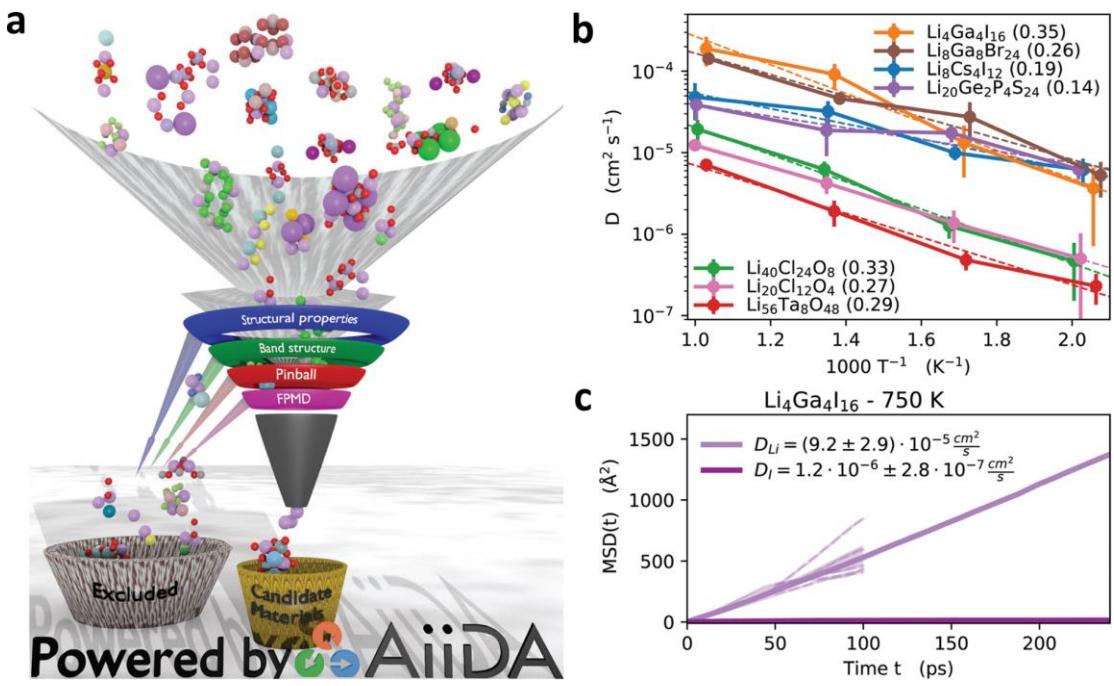


**Figure 2.** Workflow and results of the SSEs screening. a) The funnel-shaped workflow used for the SSEs screening. Reproduced with permission.[13] Copyright 2020, Royal Society of Chemistry. b) Diffusion coefficients obtained from FPMD of the well-known superionic conductor $Li_{20}Ge_2P_4S_{24}$ and the selected candidates: $Li_4Ga_4I_{16}$, $Li_7Ga_8Br_{24}$, $Li_8Cs_4I_{12}$, $Li_{40}Cl_{24}O_8$, $Li_{20}Cl_{12}O_4$, and $Li_{56}Ta_8O_{48}$. Reproduced with permission.[13] Copyright 2020, Royal Society of Chemistry. c) The MSD of Li and I at 750 K obtained from FPMD in $Li_4Ga_4I_{16}$. Reproduced with permission.[13] Copyright 2020, Royal Society of Chemistry.

## Research works using automated computational workflows

In this section, research works using automated computational workflow as the main tool will be presented. The focus will be on the research and development of battery materials, and works in other fields will also be briefly introduced.

The automated computational workflow method has been successfully applied in the field of battery materials.[13,20,39-42] Taking SSE as an example, a promising SSE material should at least meet the following five criteria: (1) electronically insulating; (2) wide electrochemical stability window and low reactivity with the anode/cathode materials; (3) high lithium ionic conductivity; (4) high elastic modulus to prevent the growth of lithium dendrites; (5) the interfaces between the SSE and the anode/cathode material cannot hinder the conduction of lithium ions.[17,18] It can be seen that judging

whether a lithium-containing compound is a qualified SSE involves a complicated workflow. Kahle et al.[13] designed a funnel-shaped automated high-throughput screening workflow to search for SSEs as illustrated in **Figure 2**a. AiiDA was used for the workflow construction and execution. From about 1,400 distinct lithium-containing compounds in the Inorganic Crystal Structure Database (ICSD)[43] and Crystallography Open Database (COD)[44] databases, five fast ion conductors, whose lithium ion diffusion coefficients are comparable to the well-known $Li_{20}Ge_2P_4S_{24}$,[45] were selected (Figure 2b). Among the five candidate materials, taking $Li_4Ga_4I_{16}$ as an example, the mean square displacement (MSD) of Li and I ions at 750 K is shown in Figure 2c. As illustrated in the red box in **Figure 3**, the screening workflow can be described as follows: (1) exclude the structures that have partial occupancies or attached hydrogen as well as the structures with rare or dangerous elements. Next (2) determine whether a lithium-containing compound is insulating. If it is an insulator, then (3) a surrogate model called the pinball model will be used to predict its lithium ion diffusion coefficient. If a high diffusion coefficient is obtained from the pinball model, then (4) first-principle molecular dynamics (FPMD) will be adopted to calculate a more accurate diffusion coefficient as the final criterion. It can be seen that this screening workflow is composed of four first-order sub-workflows connected according to a "progressive" logic (see the red box in Figure 3). Among them, the electronic band structure first-order sub-workflow can be further divided into three second-order sub-workflows, including a structure optimization, a static self-consistent field (SCF) calculation, and a static non-SCF calculation (see the blue box in Figure 3). Similarly, the structure optimization second-order sub-workflow can be further divided into four third-order sub-workflows, including writing input files, running simulation software, storing output results and passing to next workflow (see the yellow box in Figure 3). These four third-order sub-workflows can no longer be decomposed, so they are atomic-workflows. In fact, both the electronic band structure workflow and the structure optimization workflow are the most commonly used workflows, which have been encapsulated and can be directly reused. Here, in order to illustrate their structures in detail, they are expanded.

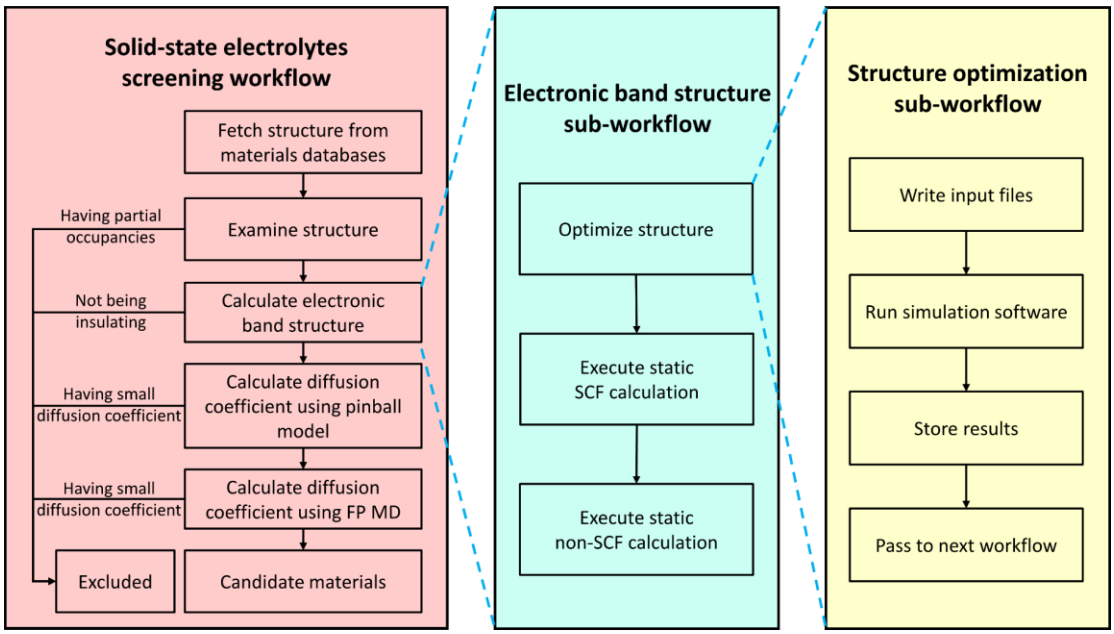


**Figure 3.** The structure of the SSEs screening workflow. The workflow in the red box refers to Ref.[13]. The workflows in the blue and yellow boxes refer to Ref.[25].

In the field of battery materials, automated computational workflow methods are not only used in the screening of SSEs, but also in the study of traditional liquid electrolytes and additives. Since liquid electrolytes are mainly composed of molecules, Halls et al.[39] designed a high-throughput workflow for the simulation of fundamental molecular properties including the highest occupied molecular orbital (HOMO) energy, lowest unoccupied molecular orbital (LUMO) energy, vertical ionization potential ($IP_v$), vertical electron affinity ($EA_v$), dipole moment, polarizability and chemical hardness. Pipeline Pilot was used for the workflow construction and execution. Using this workflow, a database of additives based on fluoro- and alkyl-derivatized ethylene carbonate (EC) was built. After a simple statistical analysis of the database, it can be found that the maximum relative $EA_v$ of fluorinated EC is 4.13 eV, which is much higher than that of alkylated EC, indicating the great improvement by including fluorine into the molecular structure.

Another work focusing on the molecular structures and properties of liquid electrolytes was conducted by Qu and co-workers.[41] Three automated workflows for the

simulation on molecules was constructed: (1) IP and EA calculation; (2) salt complex generator; (3) ion pair dissociation constant calculation. FireWorks was used for the workflow construction and execution. These workflows are well encapsulated in the Python library rubicon (https://github.com/materialsproject/rubicon) and can be used in the screening of liquid electrolytes. Among them, IP and EA are capable of determining the electrochemical window. Salt complex generator is able to predict the lowest energy complex configuration while ion pair dissociation constant can be used to compute the ion-pair formation driving force. These workflows were used in the Electrolyte Genome Project,[46] which created a molecule property database which is publicly available and integrated into the Materials Project's Explore Molecule application (https://materialsproject.org/#search/molecules).

Next, this is a multi-scale research investigating the influence of the electrolyte composition on the battery performance. In LIBs, the liquid electrolytes generally contain lithium salts, carbonate solvents and additives. Since the additives have an effect on the transport properties of the electrolyte, they will have a direct influence on the battery performance. Hanke et al.[42] constructed a multi-scale automated computational workflow which enables multi-scale simulations from electrolyte composition (type and proportion of solvent/additive, salt concentration) to electrolyte transport properties (conductivity, diffusion coefficient and transference number of lithium ions at different temperatures and salt concentrations) and to battery performance (discharge voltage profile and cell temperature profile at different temperatures and discharge rates). Pipeline Pilot was used for workflow construction and execution. The simulation from the electrolyte composition to the transport properties was achieved through MD, and the simulation from the electrolyte transport properties to the battery performance was achieved through the extended Newman model. The inputs of the workflow include electrolyte composition and simulation temperature. And the workflow can be briefly described as follows: (1) generate the structure of the electrolyte with the specified composition (about 200 solvent molecules and a specified number of lithium salts); (2) perform 100 ps MD in the NPT ensemble

at the specified temperature to thermalize the structure; (3) perform 5 ns MD in the NVE ensemble at the specified temperature to obtain the equilibrium transport properties; (4) repeat step 1 to step 3 for five times and use the averaged results to calculate the transport properties of the electrolyte; (5) pass the transport properties obtained in step 4 to the extended Newman model and simulate the battery performance. Since LIBs are the most widely used rechargeable batteries today, it is of great practical significance to design non-flammable, non-toxic and environmentally friendly liquid electrolytes for LIBs. The multi-scale workflow designed by Hanke and co-workers enables the exploration of electrolytes that meet the requirements mentioned above without compromising the battery performance.

Automated workflows have also been applied to the study of electrode materials, for example, by deciding which implementation of the NEB should be used to calculate ion diffusion barriers, depending on the material properties.[47-50] Bölle et al.[20] built an automated screening workflow for intercalation electrodes in batteries based on the calculations of volume change during charging/discharging, charge carrier adsorption energy and diffusion barriers (**Figure 4**a). MyQueue was used for workflow construction and execution. The volume change during charging/discharging can determine the stability of the electrodes. The charge carrier adsorption energy can predict the open circuit voltage and the diffusion barrier can evaluate the ion mobility at different charge states. This workflow has been tested to identify potential cathode materials for Mg-ion batteries. The volume change, the open circuit voltage and the height of diffusion barrier of $MgTi_2O_4$, $MgV_2O_4$, $MgMn_2O_4$, $Mg_3Cr_2(SiO_4)_3$, $Mg_3Mn_2(SiO_4)_3$ and the well-known Chevrel phase $MgMo_3S_4$ are shown in Figure 4b-d respectively. It can be seen that, the tested materials can further optimize the performance of the Chevrel phase, the most common cathode material in Mg-ion battery, with higher open circuit voltage and lower $Mg^{2+}$ diffusion energy barrier.

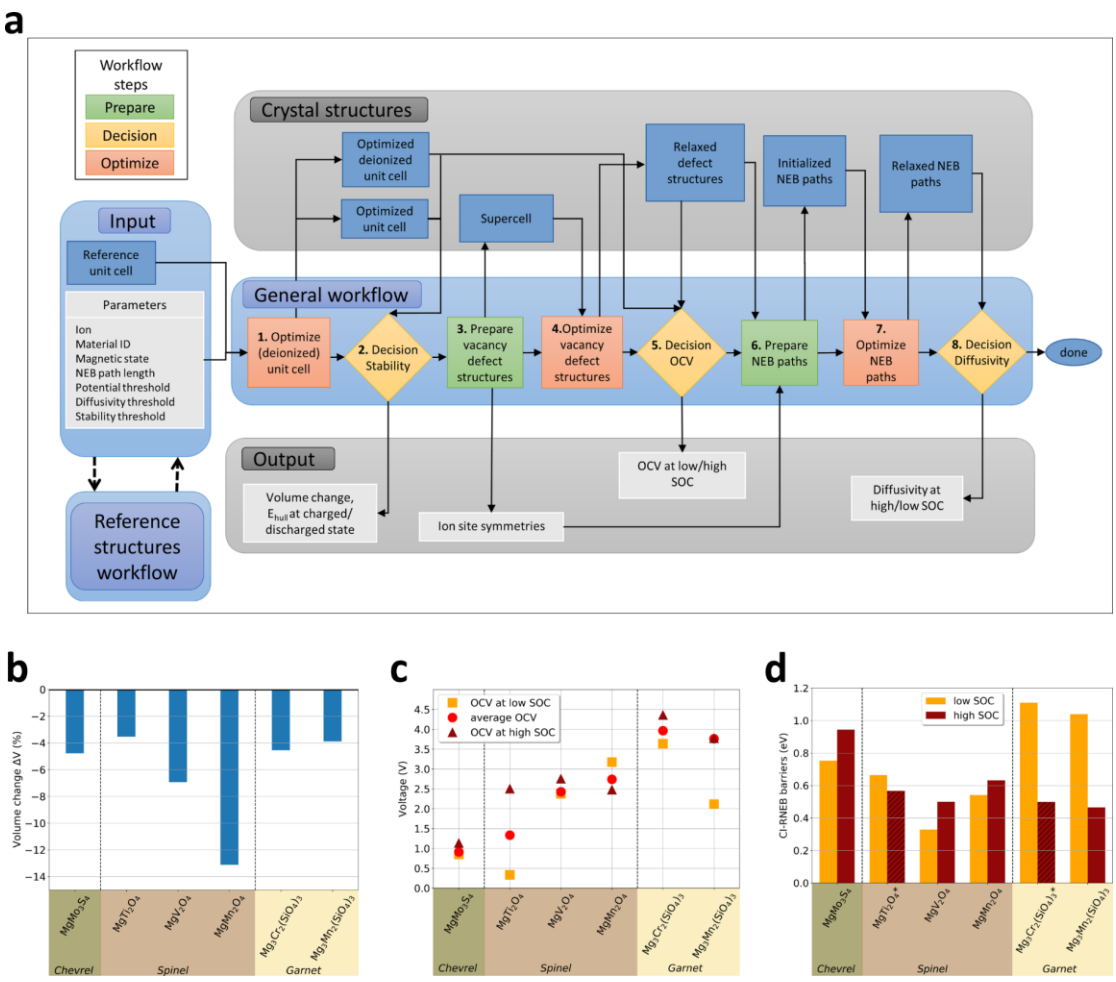


**Figure 4.** Workflow of the intercalation electrodes screening and results of the Chevrel phase and the five tested materials. a) The workflow used for the intercalation electrodes screening. Reproduced with permission.[20] Copyright 2020, Wiley-VCH Verlag GmbH & Co. KGaA, Weinheim. b) Volume change when the cathode material is charged. Reproduced with permission.[20] Copyright 2020, Wiley-VCH Verlag GmbH & Co. KGaA, Weinheim. c) OCVs at different charge states. Reproduced with permission.[20] Copyright 2020, Wiley-VCH Verlag GmbH & Co. KGaA, Weinheim. d) The height of the diffusion barrier calculated from the climbing image reflective nudged elastic bands method. Reproduced with permission.[20] Copyright 2020, Wiley-VCH Verlag GmbH & Co. KGaA, Weinheim.

Besides battery materials, the automated computational workflow method has also been applied in several other fields, such as surface science,[51,52] two-dimensional (2D) materials,[53,54] and photoelectrochemical materials.[55] Montoya et al.[51] and Tran et al.[52] constructed automated workflows to realize the high-throughput calculation of surface energy and adsorption energy. Given structures of the bulk and the adsorbate, the workflow will (1) enumerate the surfaces of the bulk and calculate the surface

energy; (2) enumerate the adsorption sites on the surface and place the adsorbate on the site to calculate the adsorption energy. Haastrup et al.[53] created more than 1,500 different 2D materials by combinatorial lattice decoration of known crystal structure prototypes. An automated workflow was then constructed to calculate various materials properties of these 2D materials, the results of which constitute the Computational 2D Materials Database (C2DB). Mounet et al.[54] designed an automated screening workflow to search for easily exfoliable layered three-dimensional (3D) materials. The workflow will detect whether a 3D material is a layered material, and if it is, the workflow will further determine whether its binding energy is small enough for exfoliation. Among 108,432 experimentally known 3D compounds downloaded from the ICSD and COD databases, 1,036 easily exfoliable candidates were selected. Kuhar et al.[55] built an automated screening workflow to search for the large-band-gap component in water splitting tandem devices. The material screening is based on the essential properties including thermodynamic stability, light absorption, charge mobility, and defect tolerance. Eight compounds were selected from 705 $ABS_3$ compounds. $LaYS_3$, a promising candidate, was successfully synthesized experimentally, confirming the effectiveness of the screening.

It can be seen that the automated computational workflow also has potential in other material fields. In fact, if a material needs to possess multiple functions, and the evaluation of these functions can be quickly realized by computational simulations, using WM to build a computational workflow to study all relevant materials in the database will be a more systematic approach. Nowadays, the complexity of material design is getting higher. Materials need to possess good intrinsic properties, and their microstructures, synthesis, prices, safety and environmental friendliness are equally important. Fortunately, simulation methods are getting more advanced, and the computing power is growing rapidly. Under such circumstances, WM, as an important tool to achieve computational high throughput, may play an important role in battery materials as well as other fields in the future.

**Future perspectives in computational workflows**

Although the automated computational workflow method has already been applied in the field of battery materials, it is still far from large-scale applications due to existing unresolved challenges. To achieve more widespread use, we propose the following research efforts and directions:

(1) At present, the material structures for high-throughput screening mainly come from mature material databases. However, there are many new materials and their metastable phases that have not been discovered. For example, Yu et al.[56] synthesized fluorinated 1,4-dimethoxylbutane (FDMB) as the electrolyte solvent. Pairing FDMB with 1 M lithium bis(fluorosulfonyl)imide, this electrolyte showed excellent performance in lithium metal batteries (LMBs). However, when the research work was reported, this simple molecule FDMB had not been included in the Chemical Abstracts Service (CAS) yet. It can be seen that some undiscovered materials may play an important role in the field of batteries. In the future, we can integrate structure prediction methods[57-62] into a workflow to find the structure with the global minimum energy of a given composition. By integrating such method, we can expand the search space for battery materials, thereby increasing the chances of finding novel battery materials. However, current structure prediction methods have difficulties in predicting large systems. Larger systems are common in battery research. Therefore, we should further develop structure prediction techniques. Structure prediction is to search for the structure corresponding to the global minimum on the potential energy surface, which is fundamentally an optimization problem. If the system to be predicted contains $N$ atoms, the dimension of the search space is $6 + 3(N - 1)$.[57] This is why the structure prediction of large system is difficult. In order to realize the structure prediction of large system, we not only have to test newly developed optimization methods, but more importantly, reduce the dimension of the search space and properly determine the boundaries of the search space according to laws of crystal structures.

(2) High-throughput screening for battery materials consumes a lot of computing

resources, especially when kinetic factors are considered.[13] Surrogate models can be adopted to achieve a trade-off between accuracy and computing cost.[52] For example, using Atomistic Machine-learning Package,[63] the potential energy surface of the studied system can be created by machine learning instead of density functional theory (DFT). The created potential energy surface can be used together with DFT to perform NEB calculations, which can greatly speed up the estimation of ionic conductivity for battery materials.[52] BVSE is another empirical method for diffusion energy barrier prediction.[64] The BVSE method was developed on the basis of the BV method, a method capable of predicting the bonding geometry and structure of a complex material. The results of the BVSE method are 3D grids, through which we can predict the ion transport path and the diffusion energy barriers. Machine learning methods can greatly improve the efficiency of MD. The machine learning force field (MLFF) created by the on-the-fly force field generation method can accelerate the MD simulation by hundreds or thousands of times compared with FPMD.[65,66] Using the MLFF, the computational cost of MD simulation only increases linearly with the system size. We can further improve the parallel efficiency of simulation software and use tools with stronger computing power such as the graphic processing unit (GPU).[67,68] In the future, we need to develop more advanced simulation methods to achieve higher accuracy while saving computing resources. For now, we can use high-accuracy (but time-consuming) advanced methods to generate training sets for training machine learning models. The obtained machine learning model can have accuracy close to advanced methods and speed close to empirical methods, such as the MLFF mentioned above. This might be a good compromise between accuracy and speed.

(3) There are only a few application scenarios of the automated workflow in the field of batteries, for example, the screening of battery materials and the construction of material property databases, and the objects are mainly bulk materials or molecules. However, the interfaces between battery materials are equally important, and many critical battery reactions occur at the interfaces between the electrode and the electrolyte, such as SEI formation and evolution, lithium dendrite growth, etc. In the future, we can

use automated computational workflow method to model and simulate the interfaces between battery materials, and attempt to explain battery mechanisms in greater detail. Compared to bulk or molecular materials, modelling of battery interfaces is much more tedious because of the large systems involved, which lends itself to automated workflows. In doing so, we also need to incorporate realistic charge and solvent effects at the interfaces, for example, by including the electrochemical potential and using implicit or explicit solvent models.[69] Machine learning is an important method for battery material research.[70,71] For machine learning, dataset construction, model selection and training are equally important. Due to the high-throughput nature of the automated computational workflow method, it is very suitable for the construction of machine learning datasets. For example, Zhao et al.[72] realized the prediction of activation energy in cubic lithium-argyrodites system by machine learning. Since a dataset containing activation energies is required to train the machine learning model, Zhao and co-workers calculated activation energies of 50 cubic lithium-argyrodites using their home-made high-throughput screening platform for solid electrolytes (SPSE)[37] automatically. This is an example of constructing machine learning dataset using automated workflow, which is encouraged in the future research.

(4) Constructing automated workflows requires programming skills. Therefore, while improving the programming ability is important, we also encourage the sharing of automated workflows. We can share our workflows in material research forums or code hosting sites like GitHub, GitLab, and SourceForge, and these workflows can be gradually improved by other researchers. When these workflows are needed, we can download and reuse them conveniently. Through AiiDA plugins, dozens of automated workflows for materials research have already been shared. This kind of co-construction and sharing model will accelerate the research and development of battery materials greatly.

**Future perspectives in experimental workflows**

In fact, automated high-throughput experiments are also needed to complement the

automated computations discussed above. In the field of battery materials, we propose the following research endeavors in the 3 main stages of materials synthesis, operando characterization and battery testing to form an automated experimental workflow (**Figure 5**):

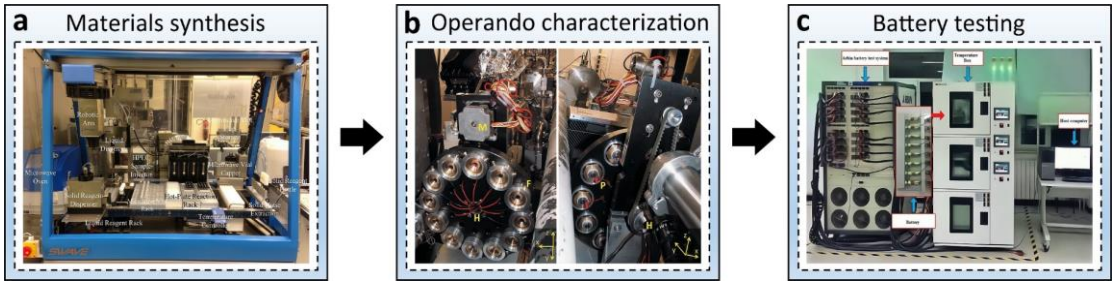


**Figure 5.** Automated experimental workflow for the research and development of battery materials. a) Materials synthesis. Reproduced with permission.[73] Copyright 2015, Society for Laboratory Automation and Screening. b) Operando characterization. Reproduced with permission.[74] Copyright 2016, International Union of Crystallography. c) Battery testing. Reproduced with permission.[75] Copyright 2020, The Authors.

(1) Combinatorial and high-throughput experimental methods have been used for rapid synthesis of materials.[76,77] Traditional synthesis methods are often performed single step at a time, which is slow and costly. With combinatorial synthesis, materials and interfaces of different chemical compositions, phases, dopants, defects, etc. can be prepared. Advanced techniques such as robotics, thin film sputtering, jet dispensing, and pulsed laser deposition can be used to synthesize and optimize such materials in a high-throughput manner (Figure 5a).[73,78-81] Using these techniques, we can also easily investigate different electrode and electrolyte materials as a function of the synthesis parameters, which allows more rapid tuning of these parameters.

Although high-throughput synthesis of battery materials has been reported, such examples are relatively scarce in the literature, which could be due to the air-sensitive nature of many electrode and electrolyte materials. In the future, we can integrate the robotic synthesis platform with a glove box and an inert gas supply, or even perform the automated synthesis in a dry room. Right now, many of the high-throughput

synthesis methods are performed on a relatively small laboratory scale. The ability to scale up the automated production of battery materials and interfaces is also of significant concern and should be further explored for practical applications.

(2) Characterization of battery materials can also be performed in an automated manner. For example, electrode materials have been studied using X-ray diffraction and X-ray absorption spectroscopy with an automated sample changer for characterization of chemical phases and local structures (Figure 5b).[74] In a similar way, one can also envision other techniques such as Raman spectroscopy being performed using an automated sample feed system with a translating/rotating sample stage to investigate the chemical composition of battery materials. For accurate characterization of battery interfaces, surface-sensitive spectroscopic techniques such as X-ray photoelectron spectroscopy (XPS) can be used to ascertain the chemical composition of interfaces as a function of depth.[82] Microscopic techniques such as transmission electron microscopy (TEM),[83] cryogenic electron microscopy[84] and scanning probe microscopy[85] can be used to study the surface topology, nanostructure and thickness of the interfaces.

The future challenge is to incorporate robotics and automation into a wider range of characterization techniques so that they can be carried out in a high-throughput manner. Examples of emerging characterization techniques include ambient-pressure XPS[86] and liquid-phase TEM,[87] which allow battery materials and interfaces to be studied more realistically in the presence of a thin film of electrolyte. Moreover, it is important to address critical issues such as formation of hot spots in liquid-phase TEM cells, which can lead to artificially enhanced electrochemical activity. High-throughput TEM is already an active area of research in biological imaging, using automation technologies such as reel-to-reel tape translation system and nano-positioning sample stage;[88,89] we hope that it can be applied to study battery materials as well.

(3) Finally, the batteries should be screened and tested in parallel in a rapid and high-

throughput manner, preferably under controlled temperature and humidity conditions (Figure 5c).[75] To perform high-throughput screening of battery materials on a small scale, one potential way is to design tiny electrochemical cells such as microfluidic cells, consisting of miniaturized components (working, counter, reference electrodes) that are integrated into a flow-based microfluidic chip.[90] On a larger scale, batteries can also be assembled using an automated production line, which involves mixing of various components (active material, conductive additive, binder), coating onto current collectors, calendering to form electrode films, slitting into appropriate dimensions, and assembly into full cells for testing (**Figure 6**).[91,92] An example of such automation technique is continuous Z-folding, where cathodes and anodes are placed alternately above and below a continuously fed separator strip before being folded in a zigzag manner using circumferential grippers.[92]

The battery testing and screening process can be further augmented using machine learning. For instance, by using big data to train a machine learning model, Severson et al. managed to use the early few test cycles to screen batteries based on low and high cycle lifetime.[93] The authors also used machine learning to optimize a parameter space specifying the current and voltage profiles of fast-charging protocols to maximize battery cycle life.[94] Future opportunities lie in improving the accuracy, explainability and generalizability of these prediction models, using state-of-the-art techniques such as explainable artificial intelligence and transfer learning.[91] The ultimate goal is to be able to integrate all these 3 components of battery materials synthesis, characterization and testing into a fully automated and continuous workflow.

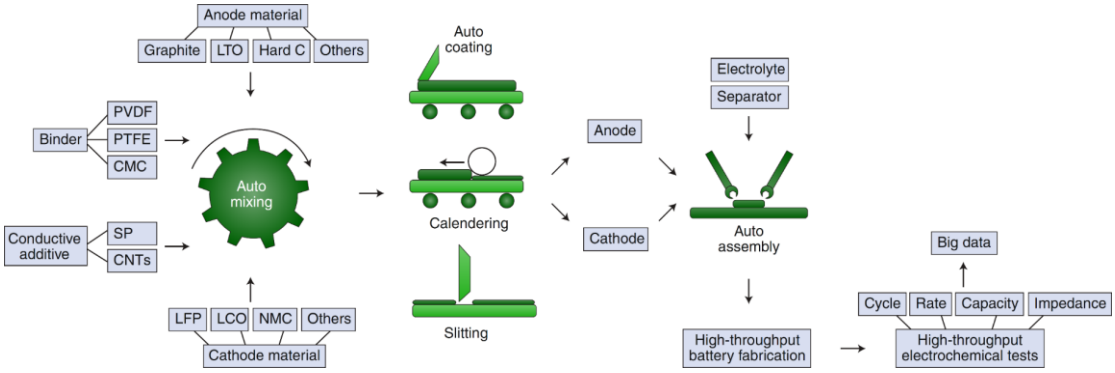


**Figure 6.** A high-throughput workflow for battery fabrication and testing. The full names of the abbreviations mentioned above are as follows. For anode material: LTO, lithium titanate; Hard C, hard carbon. For binder: PVDF, polyvinylidene fluoride; PTFE, polytetrafluoroethylene; CMC, carboxymethyl cellulose. For conductive additive: SP, super P; CNTs, carbon nanotubes. For cathode material: LFP, lithium iron phosphate; LCO, lithium cobalt oxide; NMC, lithium nickel manganese cobalt oxide. Reproduced with permission.[91] Copyright 2020, Springer Nature Limited.

## Conclusion

In conclusion, automated computational workflows have the potential to revolutionize the way we discover new battery materials and interfaces. When they are successfully integrated with automated experimental workflows, we can envision a truly closed-loop, self-driving laboratory.[95] Hopefully these concepts can be extended to a multitude of research fields to accelerate the development of new energy storage devices and beyond.

## Conflicts of interest

There are no conflicts to declare.

## Acknowledgements

Z.W.S. acknowledges the support of the Singapore National Research Foundation (NRF-NRFF2017-04) and Agency for Science, Technology and Research (Central Research Fund Award). Q.Z. was supported by the Beijing Natural Science Foundation (2192029).

## Keywords

High-throughput computations; first principles; automated workflows; machine learning; batteries

## Data availability statement

Data sharing not applicable to this article as no datasets were generated or analysed during the current study.

## References

[1] S. Chu, Y. Cui, N. Liu, *Nat. Mater.* **2017**, *16*, 16.
[2] J. B. Goodenough, K.-S. Park, *J. Am. Chem. Soc.* **2013**, *135*, 1167.
[3] M. S. Whittingham, *Chem. Rev.* **2014**, *114*, 11414.
[4] Z. W. Seh, Y. Sun, Q. Zhang, Y. Cui, *Chem. Soc. Rev.* **2016**, *45*, 5605.
[5] A. Y. S. Eng, V. Kumar, Y. Zhang, J. Luo, W. Wang, Y. Sun, W. Li, Z. W. Seh, *Adv. Energy Mater.* **2021**, *11*, 2003493.
[6] D.-T. Nguyen, R. Horia, A. Y. S. Eng, S.-W. Song, Z. W. Seh, *Mater. Horiz.* **2021**, *8*, 830.
[7] G. M. Zhou, H. Z. Tian, Y. Jin, X. Y. Tao, B. F. Liu, R. F. Zhang, Z. W. Seh, D. Zhuo, Y. Y. Liu, J. Sun, J. Zhao, C. X. Zu, D. S. Wu, Q. F. Zhang, Y. Cui, *Proc. Natl. Acad. Sci. U. S. A.* **2017**, *114*, 840.
[8] W. W. Yang, J. W. Xiao, Y. Ma, S. Q. Cui, P. Zhang, P. B. Zhai, L. J. Meng, X. G. Wang, Y. Wei, Z. G. Du, B. X. Li, Z. B. Sun, S. B. Yang, Q. F. Zhang, Y. J. Gong, *Adv. Energy Mater.* **2019**, *9*, 1803137.
[9] J. Yu, J. W. Xiao, A. R. Li, Z. Yang, L. Zeng, Q. F. Zhang, Y. J. Zhu, L. Guo, *Angew. Chem., Int. Ed.* **2020**, *59*, 13071.
[10] G. M. Zhou, S. Y. Wang, T. S. Wang, S. Z. Yang, B. Johannessen, H. Chen, C. W. Liu, Y. S. Ye, Y. C. Wu, Y. C. Peng, C. Liu, S. P. Jiang, Q. F. Zhang, Y. Cui, *Nano Lett.* **2020**, *20*, 1252.
[11] T. S. Wang, P. B. Zhai, D. Legut, L. Wang, X. P. Liu, B. X. Li, C. X. Dong, Y. C. Fan, Y. J. Gong, Q. F. Zhang, *Adv. Energy Mater.* **2019**, *9*, 1804000.
[12] P. B. Zhai, T. S. Wang, W. W. Yang, S. Q. Cui, P. Zhang, A. M. Nie, Q. F. Zhang, Y. J. Gong, *Adv. Energy Mater.* **2019**, *9*, 1804019.
[13] L. Kahle, A. Marcolongo, N. Marzari, *Energy Environ. Sci.* **2020**, *13*, 928.
[14] H. Z. Tian, Z. W. Seh, K. Yan, Z. H. Fu, P. Tang, Y. Y. Lu, R. F. Zhang, D. Legut, Y. Cui, Q. F. Zhang, *Adv. Energy Mater.* **2017**, *7*, 1602528.
[15] J. G. Zhu, P. K. Li, X. Chen, D. Legut, Y. C. Fan, R. F. Zhang, Y. Y. Lu, X. B. Cheng, Q. F. Zhang, *Energy Storage Mater.* **2019**, *16*, 426.
[16] J. Liang, Z.-H. Sun, F. Li, H.-M. Cheng, *Energy Storage Mater.* **2016**, *2*, 76.
[17] Q. Zhao, S. Stalin, C.-Z. Zhao, L. A. Archer, *Nat. Rev. Mater.* **2020**, *5*, 229.
[18] Y. Xiao, Y. Wang, S.-H. Bo, J. C. Kim, L. J. Miara, G. Ceder, *Nat. Rev. Mater.* **2020**, *5*, 105.

[19] P. G. Bruce, S. A. Freunberger, L. J. Hardwick, J. M. Tarascon, *Nat. Mater.* **2012**, *11*, 19.
[20] F. T. Bölle, N. R. Mathiesen, A. J. Nielsen, T. Vegge, J. M. Garcia-Lastra, I. E. Castelli, *Batteries Supercaps* **2020**, *3*, 488.
[21] J. H. Montoya, K. T. Winther, R. A. Flores, T. Bligaard, J. S. Hummelshoj, M. Aykol, *Chem. Sci.* **2020**, *11*, 8517.
[22] W. Y. Li, Q. F. Zhang, G. Y. Zheng, Z. W. Seh, H. B. Yao, Y. Cui, *Nano Lett.* **2013**, *13*, 5534.
[23] Z. W. Seh, H. T. Wang, P. C. Hsu, Q. F. Zhang, W. Y. Li, G. Y. Zheng, H. B. Yao, Y. Cui, *Energy Environ. Sci.* **2014**, *7*, 672.
[24] Z. W. Seh, J. H. Yu, W. Y. Li, P. C. Hsu, H. T. Wang, Y. M. Sun, H. B. Yao, Q. F. Zhang, Y. Cui, *Nat. Commun.* **2014**, *5*, 5017.
[25] K. Mathew, J. H. Montoya, A. Faghaninia, S. Dwarakanath, M. Aykol, H. Tang, I.-h. Chu, T. Smidt, B. Bocklund, M. Horton, J. Dagdelen, B. Wood, Z.-K. Liu, J. Neaton, S. P. Ong, K. Persson, A. Jain, *Comput. Mater. Sci.* **2017**, *139*, 140.
[26] S. P. Huber, S. Zoupanos, M. Uhrin, L. Talirz, L. Kahle, R. Haeuselmann, D. Gresch, T. Mueller, A. V. Yakutovich, C. W. Andersen, F. F. Ramirez, C. S. Adorf, F. Gargiulo, S. Kumbhar, E. Passaro, C. Johnston, A. Merkys, A. Cepellotti, N. Mounet, N. Marzari, B. Kozinsky, G. Pizzi, *Sci. Data* **2020**, *7*, 300.
[27] M. Uhrin, S. P. Huber, J. Yu, N. Marzari, G. Pizzi, *Comput. Mater. Sci.* **2021**, *187*, 110086.
[28] C. E. Calderon, J. J. Plata, C. Toher, C. Oses, O. Levy, M. Fornari, A. Natan, M. J. Mehl, G. Hart, M. B. Nardelli, S. Curtarolo, *Comput. Mater. Sci.* **2015**, *108*, 233.
[29] S. Curtarolo, W. Setyawan, G. L. W. Hart, M. Jahnatek, R. V. Chepulskii, R. H. Taylor, S. Wanga, J. Xue, K. Yang, O. Levy, M. J. Mehl, H. T. Stokes, D. O. Demchenko, D. Morgan, *Comput. Mater. Sci.* **2012**, *58*, 218.
[30] J. J. Mortensen, M. Gjerding, K. S. Thygesen, *J. Open Source Softw.* **2020**, *5*, 1844.
[31] S. P. Ong, W. D. Richards, A. Jain, G. Hautier, M. Kocher, S. Cholia, D. Gunter, V. L. Chevrier, K. A. Persson, G. Ceder, *Comput. Mater. Sci.* **2013**, *68*, 314.
[32] A. Jain, S. P. Ong, W. Chen, B. Medasani, X. Qu, M. Kocher, M. Brafman, G. Petretto, G.-M. Rignanese, G. Hautier, D. Gunter, K. A. Persson, *Concurr. Comput. Pract. Exp.* **2015**, *27*, 5037.
[33] A. Jain, S. P. Ong, G. Hautier, W. Chen, W. D. Richards, S. Dacek, S. Cholia, D. Gunter, D. Skinner, G. Ceder, K. A. Persson, *APL Mater.* **2013**, *1*, 011002.
[34] S. Curtarolo, W. Setyawan, S. Wang, J. Xue, K. Yang, R. H. Taylor, L. J. Nelson, G. L. W. Hart, S. Sanvito, M. Buongiorno-Nardelli, N. Mingo, O. Levy, *Comput. Mater. Sci.* **2012**, *58*, 227.
[35] B. He, P. H. Mi, A. J. Ye, S. T. Chi, Y. Jiao, L. W. Zhang, B. W. Pu, Z. Y. Zou, W. Q. Zhang, M. Avdeev, S. Adams, J. T. Zhao, S. Q. Shi, *Acta Mater.* **2021**, *203*, 116490.
[36] L. Pan, L. W. Zhang, A. J. Ye, S. T. Chi, Z. Y. Zou, B. He, L. L. Chen, Q. Zhao, D. Wang, S. Q. Shi, *J. Materiomics* **2019**, *5*, 688.
[37] B. He, S. T. Chi, A. J. Ye, P. H. Mi, L. W. Zhang, B. W. Pu, Z. Y. Zou, Y. B. Ran, Q. Zhao, D. Wang, W. Q. Zhang, J. T. Zhao, S. Adams, M. Avdeev, S. Q. Shi, *Sci. Data* **2020**, *7*, 151.

[38] B. He, A. J. Ye, S. T. Chi, P. H. Mi, Y. B. Ran, L. W. Zhang, X. X. Zou, B. W. Pu, Q. Zhao, Z. Y. Zou, D. Wang, W. Q. Zhang, J. T. Zhao, M. Avdeev, S. Q. Shi, *Sci. Data* **2020**, *7*, 153.
[39] M. D. Halls, K. Tasaki, *J. Power Sources* **2010**, *195*, 1472.
[40] N. A. Katcho, J. Carrete, M. Reynaud, G. Rousse, M. Casas-Cabanas, N. Mingo, J. Rodriguez-Carvajal, J. Carrasco, *J. Appl. Crystallogr.* **2019**, *52*, 148.
[41] X. Qu, A. Jain, N. N. Rajput, L. Cheng, Y. Zhang, S. P. Ong, M. Brafman, E. Maginn, L. A. Curtiss, K. A. Persson, *Comput. Mater. Sci.* **2015**, *103*, 56.
[42] F. Hanke, N. Modrow, R. L. C. Akkermans, I. Korotkin, F. C. Mocanu, V. A. Neufeld, M. Veit, *J. Electrochem. Soc.* **2019**, *167*, 013522.
[43] A. Belsky, M. Hellenbrandt, V. L. Karen, P. Luksch, *Acta Crystallogr. Sect. B Struct. Sci.* **2002**, *58*, 364.
[44] S. Grazulis, A. Daskevic, A. Merkys, D. Chateigner, L. Lutterotti, M. Quiros, N. R. Serebryanaya, P. Moeck, R. T. Downs, A. Le Bail, *Nucleic Acids Res.* **2012**, *40*, D420.
[45] N. Kamaya, K. Homma, Y. Yamakawa, M. Hirayama, R. Kanno, M. Yonemura, T. Kamiyama, Y. Kato, S. Hama, K. Kawamoto, A. Mitsui, *Nat. Mater.* **2011**, *10*, 682.
[46] L. Cheng, R. S. Assary, X. H. Qu, A. Jain, S. P. Ong, N. N. Rajput, K. Persson, L. A. Curtiss, *J. Phys. Chem. Lett.* **2015**, *6*, 283.
[47] D. Sheppard, R. Terrell, G. Henkelman, *J. Chem. Phys.* **2008**, *128*, 134106.
[48] Z. Rong, D. Kitchaev, P. Canepa, W. Huang, G. Ceder, *J. Chem. Phys.* **2016**, *145*, 074112.
[49] E. L. Kolsbjerg, M. N. Groves, B. Hammer, *J. Chem. Phys.* **2016**, *145*, 094107.
[50] N. R. Mathiesen, H. Jonsson, T. Vegge, J. M. G. Lastra, *J. Chem. Theory Comput.* **2019**, *15*, 3215.
[51] J. H. Montoya, K. A. Persson, *npj Comput. Mater.* **2017**, *3*, 14.
[52] K. Tran, A. Palizhati, S. Back, Z. W. Ulissi, *J. Chem. Inf. Model.* **2018**, *58*, 2392.
[53] S. Haastrup, M. Strange, M. Pandey, T. Deilmann, P. S. Schmidt, N. F. Hinsche, M. N. Gjerding, D. Torelli, P. M. Larsen, A. C. Riis-Jensen, J. Gath, K. W. Jacobsen, J. J. Mortensen, T. Olsen, K. S. Thygesen, *2D Mater.* **2018**, *5*, 042002.
[54] N. Mounet, M. Gibertini, P. Schwaller, D. Campi, A. Merkys, A. Marrazzo, T. Sohier, I. E. Castelli, A. Cepellotti, G. Pizzi, N. Marzari, *Nat. Nanotechnol.* **2018**, *13*, 246.
[55] K. Kuhar, A. Crovetto, M. Pandey, K. S. Thygesen, B. Seger, P. C. K. Vesborg, O. Hansen, I. Chorkendorff, K. W. Jacobsen, *Energy Environ. Sci.* **2017**, *10*, 2579.
[56] Z. Yu, H. Wang, X. Kong, W. Huang, Y. Tsao, D. G. Mackanic, K. Wang, X. Wang, W. Huang, S. Choudhury, Y. Zheng, C. V. Amanchukwu, S. T. Hung, Y. Ma, E. G. Lomeli, J. Qin, Y. Cui, Z. Bao, *Nat. Energy* **2020**, *5*, 526.
[57] C. W. Glass, A. R. Oganov, N. Hansen, *Comput. Phys. Commun.* **2006**, *175*, 713.
[58] X. Cao, Y. Fan, J. Qu, T. Wang, D. Legut, Q. Zhang, *J. Energy Chem.* **2020**, *47*, 160.
[59] C. J. Pickard, R. J. Needs, *J. Phys.: Condens. Matter* **2011**, *23*, 053201.
[60] J. Xiao, G. Zhou, H. Chen, X. Feng, D. Legut, Y. Fan, T. Wang, Y. Cui, Q. Zhang, *Nano Lett.* **2019**, *19*, 7487.
[61] Y. Wang, J. Lv, L. Zhu, Y. Ma, *Phys. Rev. B* **2010**, *82*, 094116.

[62] X. Wang, R. Xiao, H. Li, L. Chen, *Phys. Rev. Lett.* **2017**, *118*, 195901.
[63] A. Khorshidi, A. A. Peterson, *Comput. Phys. Commun.* **2016**, *207*, 310.
[64] S. Adams, R. P. Rao, *Phys. Status Solidi A* **2011**, *208*, 1746.
[65] R. Jinnouchi, F. Karsai, G. Kresse, *Phys. Rev. B* **2019**, *100*, 014105.
[66] R. Jinnouchi, J. Lahnsteiner, F. Karsai, G. Kresse, M. Bokdam, *Phys. Rev. Lett.* **2019**, *122*, 225701.
[67] W. Jia, Z. Cao, L. Wang, J. Fu, X. Chi, W. Gao, L.-W. Wang, *Comput. Phys. Commun.* **2013**, *184*, 9.
[68] W. Jia, J. Fu, Z. Cao, L. Wang, X. Chi, W. Gao, L.-W. Wang, *J. Comput. Phys.* **2013**, *251*, 102.
[69] S. N. Steinmann, Z. W. Seh, *Nat. Rev. Mater.* **2021**, *6*, 289.
[70] Y. Liu, T. L. Zhao, W. W. Ju, S. Q. Shi, *J. Materiomics* **2017**, *3*, 159.
[71] Y. Liu, B. R. Guo, X. X. Zou, Y. J. Li, S. Q. Shi, *Energy Storage Mater.* **2020**, *31*, 434.
[72] Q. Zhao, L. W. Zhang, B. He, A. J. Ye, M. Avdeev, L. Q. Chen, S. Q. Shi, *Energy Storage Mater.* **2021**, *40*, 386.
[73] N. P. Tu, P. A. Searle, K. Sarris, *J. Lab. Autom.* **2016**, *21*, 459.
[74] J. Sottmann, R. Homs-Regojo, D. S. Wragg, H. Fjellvag, S. Margadonna, H. Emerich, *J. Appl. Crystallogr.* **2016**, *49*, 1972.
[75] J. Li, M. Ye, W. Meng, X. Xu, S. Jiao, *IEEE Access* **2020**, *8*, 195398.
[76] X. D. Xiang, X. Sun, G. Briceno, Y. Lou, K. A. Wang, H. Chang, W. G. Wallace-Freedman, S. W. Chen, P. G. Schultz, *Science* **1995**, *268*, 1738.
[77] A. Kafizas, I. P. Parkin, *Chem. Soc. Rev.* **2012**, *41*, 738.
[78] M. Roberts, J. Owen, *ACS Comb. Sci.* **2011**, *13*, 126.
[79] S. Maruyama, O. Kubokawa, K. Nanbu, K. Fujimoto, Y. Matsumoto, *ACS Comb. Sci.* **2016**, *18*, 343.
[80] S. Matsuda, K. Nishioka, S. Nakanishi, *Sci. Rep.* **2019**, *9*, 6211.
[81] T. Adhikari, A. Hebert, M. Adamic, J. Yao, K. Potts, E. McCalla, *ACS Comb. Sci.* **2020**, *22*, 311.
[82] V. Kumar, Y. Wang, A. Y. S. Eng, M.-F. Ng, Z. W. Seh, *Cell Rep. Phys. Sci.* **2020**, *1*, 100044.
[83] Z. Zeng, W.-I. Liang, H.-G. Liao, H. L. Xin, Y.-H. Chu, H. Zheng, *Nano Lett.* **2014**, *14*, 1745.
[84] Y. Li, Y. Li, A. Pei, K. Yan, Y. Sun, C.-L. Wu, L.-M. Joubert, R. Chin, A. L. Koh, Y. Yu, J. Perrino, B. Butz, S. Chu, Y. Cui, *Science* **2017**, *358*, 506.
[85] R. Kempaiah, G. Vasudevamurthy, A. Subramanian, *Nano Energy* **2019**, *65*, 103925.
[86] E. J. Crumlin, H. Bluhm, Z. Liu, *J. Electron Spectrosc. Relat. Phenom.* **2013**, *190*, 84.
[87] F. Wu, N. Yao, *Nano Energy* **2015**, *11*, 196.
[88] B. J. Graham, D. G. C. Hildebrand, A. T. Kuan, J. T. Maniates-Selvin, L. A. Thomas, B. L. Shanny, W.-C. A. Lee, *Biorxiv* **2019**, 657346.
[89] W. J. Yin, D. Brittain, J. Borseth, M. E. Scott, D. Williams, J. Perkins, C. S. Own, M. Murfitt, R. M. Torres, D. Kapner, G. Mahalingam, A. Bleckert, D. Castelli, D. Reid,

W. C. A. Lee, B. J. Graham, M. Takeno, D. J. Bumbarger, C. Farrell, R. C. Reid, N. M. da Costa, *Nat. Commun.* **2020**, *11*, 4949.
[90] J. W. Lee, M.-A. Goulet, E. Kjeang, *Lab Chip* **2013**, *13*, 2504.
[91] M.-F. Ng, J. Zhao, Q. Yan, G. J. Conduit, Z. W. Seh, *Nat. Mach. Intell.* **2020**, *2*, 161.
[92] A. Kwade, W. Haselrieder, R. Leithoff, A. Modlinger, F. Dietrich, K. Droeder, *Nat. Energy* **2018**, *3*, 290.
[93] K. A. Severson, P. M. Attia, N. Jin, N. Perkins, B. Jiang, Z. Yang, M. H. Chen, M. Aykol, P. K. Herring, D. Fraggedakis, M. Z. Bazan, S. J. Harris, W. C. Chueh, R. D. Braatz, *Nat. Energy* **2019**, *4*, 383.
[94] P. M. Attia, A. Grover, N. Jin, K. A. Severson, T. M. Markov, Y.-H. Liao, M. H. Chen, B. Cheong, N. Perkins, Z. Yang, P. K. Herring, M. Aykol, S. J. Harris, R. D. Braatz, S. Ermon, W. C. Chueh, *Nature* **2020**, *578*, 397.
[95] D. P. Tabor, L. M. Roch, S. K. Saikin, C. Kreisbeck, D. Sheberla, J. H. Montoya, S. Dwaraknath, M. Aykol, C. Ortiz, H. Tribukait, C. Amador-Bedolla, C. J. Brabec, B. Maruyama, K. A. Persson, A. Aspuru-Guzik, *Nat. Rev. Mater.* **2018**, *3*, 5.

## Biographies

Xiang Feng received his B.S. degree from Beihang University in 2019. He is currently pursuing a Ph.D. degree in Beihang University. His current research focus on the theoretical simulation of functional materials for lithium-sulfur batteries under the supervision of Prof. Qianfan Zhang.

Qianfan Zhang joined Beihang University as a faculty member in 2013. He received his Ph.D. degree from the Institute of Physics, Chinese Academy of Sciences in 2010 (with Prof. Enge Wang) and went to Stanford University for his postdoctoral research from 2010 to 2012 (with Prof. Yi Cui). His research interests have focused on the theoretical design on lithium (sodium) battery electrode materials and two-dimensional materials.

Zhi Wei Seh is a Senior Scientist at the Institute of Materials Research and Engineering, A*STAR. He received his BS and PhD degrees in Materials Science and Engineering from Cornell University and Stanford University, respectively. His research interests lie in the design of new materials for energy storage and conversion, including advanced batteries and electrocatalysts. As a Highly Cited Researcher on Web of Science, he is widely recognized for designing the first yolk-shell nanostructure in lithium-sulfur batteries.